



In silico analysis of exercise intolerance in myalgic encephalomyelitis/chronic fatigue syndrome

Nicor Lengert*, Barbara Drossel

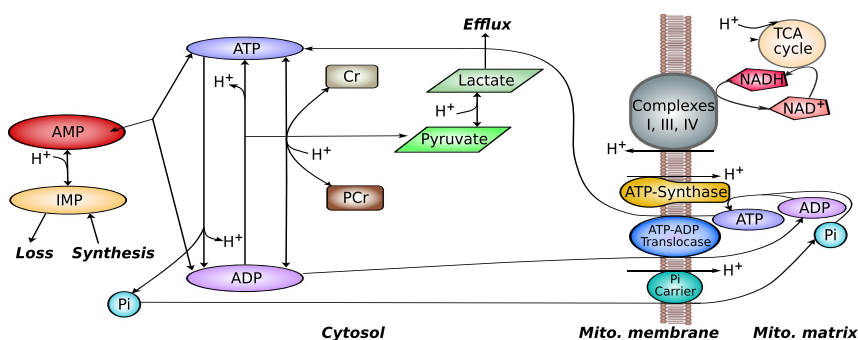
Institute for Condensed Matter Physics, Technische Universität Darmstadt, Hochschulstr. 6, 64289 Darmstadt, Germany



HIGHLIGHTS

- Metabolite dynamics in skeletal muscles are simulated during high intensity exercise.
- We take into account exercise induced purine nucleotide loss and de novo synthesis.
- A reduced mitochondrial capacity is assumed for CFS patients.
- CFS simulations exhibit critically low levels of ATP and a prolonged recovery time.
- Additionally an increased acidosis and lactate accumulation is observed in CFS.

GRAPHICAL ABSTRACT



ARTICLE INFO

Article history:

Received 23 February 2015
Received in revised form 26 March 2015
Accepted 28 March 2015
Available online 4 April 2015

Keywords:

Myalgic encephalomyelitis
Chronic fatigue syndrome
Post-exertional malaise
Exercise intolerance
ATP synthesis
Exercise recovery

ABSTRACT

Post-exertional malaise is commonly observed in patients with myalgic encephalomyelitis/chronic fatigue syndrome, but its mechanism is not yet well understood. A reduced capacity for mitochondrial ATP synthesis is associated with the pathogenesis of CFS and is suspected to be a major contribution to exercise intolerance in CFS patients. To demonstrate the connection between a reduced mitochondrial capacity and exercise intolerance, we present a model which simulates metabolite dynamics in skeletal muscles during exercise and recovery. CFS simulations exhibit critically low levels of ATP, where an increased rate of cell death would be expected. To stabilize the energy supply at low ATP concentrations the total adenine nucleotide pool is reduced substantially causing a prolonged recovery time even without consideration of other factors, such as immunological dysregulations and oxidative stress. Repeated exercises worsen this situation considerably. Furthermore, CFS simulations exhibited an increased acidosis and lactate accumulation consistent with experimental observations.

© 2015 Elsevier B.V. All rights reserved.

1. Introduction

Myalgic encephalomyelitis, also referred to as chronic fatigue syndrome (CFS), is characterized by a persistent debilitating fatigue and a variety of other symptoms with an as yet unidentified pathogenesis.

Since no simple and unambiguous diagnostic tests exist and CFS patients often do not feature a sickly appearance it was mostly treated as a psychosocial disorder. But recent studies published in the last two decades repeatedly demonstrated evidence for physical abnormalities [1–14] indicating a complex organic dysfunction. Cognitive behavioral therapy and graded exercise, which are often used to treat depression, have been reported to be ineffective or even harmful to CFS patients [15–17]. Exacerbation of the symptoms even after minimal exercise is a common feature among CFS patients, referred to as post-exertional

* Corresponding author.

E-mail address: nicor@fkp.tu-darmstadt.de (N. Lengert).

malaise (PEM), which includes increased fatigue, muscular pain, headache, nausea, and physical weakness [10,11]. Post-exertional malaise was found to be linked to an increased oxidative stress [12] and to immunological and adrenergic dysregulations that persisted for up to 48 h after exertion [18,19]. Oxidative stress is not only induced after exercise, but was shown to be also present in rest and associated with CFS symptoms [7–9].

Even though PEM is considered only as an optional symptom in the criteria for CFS by Fukuda et al. [20], it was included into later definitions of CFS as a requirement [21,22]. The most recent redefinition by the Institute of Medicine of the National Academies regards PEM as the second most essential symptom and proposes the term “systemic exertion intolerance disease” for CFS to include its importance [22].

To investigate further into the commonly observed exercise intolerance in CFS patients, studies about the performance during exercise were carried out reporting that the maximal peak work, peak O_2 uptake and the aerobic ATP synthesis rate were significantly lower in CFS patients compared to controls [1–4,14]. In other studies there was no clear distinction between the groups during the exercise test. However a second test, repeated after 24 h, resulted in a conclusive differentiation [23,24], consistent with the worsening of the medical condition due to post-exertional malaise. Furthermore an increased acidification, a reduced anaerobic threshold and a prolonged pH recovery have been reported [1,25], suggesting a compensatory upregulation of anaerobic ATP synthesis.

The reduced rate of aerobic ATP synthesis indicates a deficiency of the mitochondrial oxidative phosphorylation, which could be related to the observations of unusual mitochondrial DNA deletions in CFS patients [13]. There is also preliminary evidence for alterations in gene transcripts affecting mitochondrial functions after Epstein Barr virus infection [26], which is associated with the pathogenesis of CFS [27], although there is no conclusive evidence for the identification of a single virus as the trigger of CFS. Still, the often reported onset of CFS after a viral infection emphasizes the role of dysregulation in the immunological response to viruses in the pathogenesis of CFS [27].

Part of the dysregulation is a chronic immune activation with high elastase and RNase L activities and elevated concentration of proinflammatory cytokines such as IFN- γ and TNF- α , which have been shown to decrease the capacity of mitochondrial respiration [27,28]. It was also confirmatively reported that the elastase and RNase L activities correlate with the severity of exercise intolerance in CFS patients [29].

In order to demonstrate the effects of a reduced mitochondrial capacity on the exercise response and to predict the recovery time in CFS patients, we present a model to simulate the metabolite concentrations during high intensity exercise. The model is based on an existing model of oxidative phosphorylation and glycolysis in skeletal muscle by Korzeniewski et al. [30,31]. The original model has been demonstrated to have a similar qualitative behavior as experimental observations [32,33,30,31]. Moreover, other models integrating the model of Korzeniewski et al. proved to be consistent with experimental data in the special case of cyclic excitation in heart cells [34,35]. But neither has been tested against the literature data of several independent measurements after high intensity exercise yet. Furthermore, the purine nucleotide degradation and subsequent loss has not been considered before, therefore the models mentioned above were not able to explain the increased fatigue and prolonged recovery time after intermittent training or high intensity exercise.

Extending the original model, we also include the lactate accumulation, a more detailed description of acidosis and the purine nucleotide degradation during exercise and de novo synthesis during recovery. Thus, we are able to investigate into the mechanisms influencing the exercise response and show that the duration of recovery is prolonged considerably in CFS patients, especially for repeated exercise scenarios. Additionally, the model predictions demonstrate how a reduced mitochondrial capacity alone, without consideration of other pathological factors, is sufficient to explain some of the main symptoms of PEM

caused by low ATP levels during recovery, subsequent higher apoptosis rates and increased acidification of muscle tissue after exertion.

2. Methods

We extended an existing model of oxidative phosphorylation and glycolysis by Korzeniewski et al. [30,31] to perform computer simulations which reproduce exercise dynamics close to the experimental observations. As described in [30], the model space consists of two compartments, the cytosolic space and the mitochondrial matrix, separated by the inner mitochondrial membrane with specific carrier enzymes for the exchange of species and a volume ratio between inner and outer compartment of 1:15 [30,31]. The outer mitochondrial membrane and the intermembrane space are not included. An overview of the species interactions is depicted in Fig. 1. These interactions were included because of their major influence on the metabolite dynamics during muscle exertion and recovery.

Eqs. (1a)–(1o) determine the time evolution of the system. Reactions species and mathematical expressions not included in the original model of Korzeniewski et al. [30,31] are marked in boldface. The equations of all reaction velocities are shown in Table 1 with additional explanatory remarks in the following three sections.

$$\partial_t \text{ATP}_e = v_{EX} - v_{UT} + v_{AK} + v_{CK} + 1.5 \cdot v_{glyc} - v_{AS} - 5 \cdot v_{IS}, \quad (1a)$$

$$\partial_t \text{ADP}_e = -v_{EX} + v_{UT} - 2 \cdot v_{AK} - v_{CK} - 1.5 \cdot v_{glyc} + v_{AS} + 4 \cdot v_{IS}, \quad (1b)$$

$$\partial_t \text{AMP} = v_{AK} + v_{AS} - v_{AD} + v_{IS}, \quad (1c)$$

$$\partial_t \text{IMP} = -v_{AS} + v_{AD} - v_{PL} + v_{IS}, \quad (1d)$$

$$\partial_t \text{Pi}_e = v_{UT} - v_{PI} - 1.5 \cdot v_{glyc} + v_{AS} + 6 \cdot v_{IS}, \quad (1e)$$

$$\partial_t \text{pyruvate} = v_{glyc} - v_{DH}/5.6 - v_{LA}, \quad (1f)$$

$$\partial_t \text{lactate} = v_{LA} - v_{LE}, \quad (1g)$$

$$\partial_t \text{PCr} = -v_{CK}, \quad (1h)$$

$$\begin{aligned} \partial_t H_e^+ = & (4 + 4u)v_{C4} + (4 - 2u)v_{C3} + 4v_{C1} - n_A \cdot v_{SN} - u \cdot v_{EX} \\ & - (1 - u)v_{PI} - (1 - R_{H_2PO_4})v_{PI} - v_{CK} - v_{PE} - v_{LK} - v_{LA} \\ & + (2 - R_{H_2PO_4})v_{AS} - v_{AD} + (1 - R_{H_2PO_4})(v_{UT} + 6 \cdot v_{IS}) \\ & + (0.5 + 1.5 \cdot R_{H_2PO_4}) \cdot (v_{glyc} - v_{DH}/5.6), \end{aligned} \quad (1i)$$

$$\begin{aligned} \partial_t H_i^+ = & -15((4 + 4u)v_{C4} + (4 - 2u)v_{C3} + 4v_{C1} - n_A \cdot v_{SN} \\ & - u \cdot v_{EX} - (1 - u)v_{PI} - (1 - R_{H_2PO_4})v_{PI} \\ & - v_{LK} + (1 - R_{H_2PO_4})v_{SN}), \end{aligned} \quad (1j)$$

$$\partial_t \text{ATP}_i = 15(v_{SN} - v_{EX}), \quad (1k)$$

$$\partial_t \text{Pi}_i = 15(v_{PI} - v_{SN}), \quad (1l)$$

$$\partial_t \text{NAHD} = 15(v_{DH} - v_{C1})/5, \quad (1m)$$

$$\partial_t \text{UQH}_2 = 15(v_{C1} - v_{C3}), \quad (1n)$$

$$\partial_t C^{2+} = 15(v_{C3} - 2 \cdot v_{C4}). \quad (1o)$$

2.1. Intramitochondrial reactions

The tricarboxylic acid cycle and the transport of pyruvate and other associated metabolites through the inner mitochondrial membrane are modeled by a simple phenomenological equation for the production of

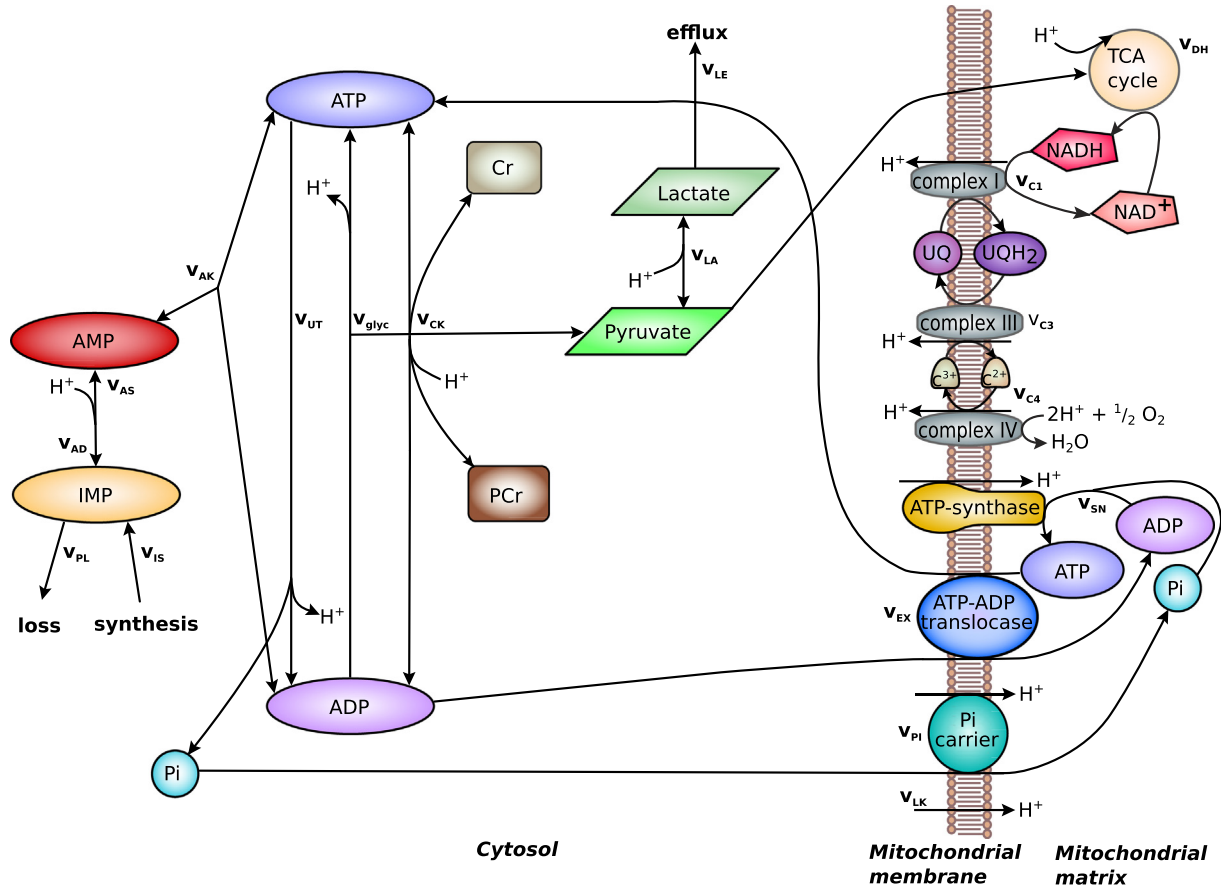


Fig. 1. Interaction diagram. The reaction directions are indicated as arrows. The ratio between the mitochondrial matrix volume and the cytosolic compartment is assumed to be 1:15 [30,31].

NADH as described in [30], but with an additional dependence on the pyruvate concentration. The ratios between the fluxes of dehydrogenase, the mitochondrial complexes, the ATP synthesis and glycolysis were determined under the following conditions: The ATP yield per NADH was assumed to be 2.5 [36] and the number of NADH gained per glycogen during oxidative phosphorylation was set to $10 + 2 \cdot 0.6 = 11.2$, since 10 NADH and 2 FADH_2 are formed, where the ATP yield of FADH_2 equals 60% of the ATP yield per NADH [36]. Thus 28 ATP are obtained per glycogen via oxidative phosphorylation and 3 ATP during the preceding glycolysis. The equations for the mitochondrial complexes I–III and the ATP synthase are taken from [30]; however, the kinetic constants are adjusted to fulfill the steady state conditions for realistic intramitochondrial concentrations, redox ratios (see Table 2) and flux ratios mentioned above.

2.2. Extramitochondrial reactions

For simplicity the glycolytic flux is modeled only as ADP and pH dependent, which is a good approximation to the complex glycolytic regulation [31].

To take into account the effect of purine nucleotide loss during exercise we included the AMP deaminase and the subsequent degradation of IMP. Measurements of the AMP deaminase activity revealed about a twofold increase when the pH is reduced from 7.0 to 6.5 [37], which is modeled as a linear function. The regulation of AMP deaminase is modeled by a dependence of the K_m value on the concentrations of free ADP and phosphate, since ADP is known for its activating and phosphate for its inhibitory effect [38,37,39]. Furthermore, the binding to myosin was found to reduce the K_m value 20 fold [40] and the amount

of bound AMP deaminase ranges from 10–60% depending on the stimulation of the muscle [41]. As an approximation of the mean effect the K_m is divided by r_{myo} , which reaches up to a value of 11 for high workloads. It was reported that some of the accumulated IMP is degraded to inosine and hypoxanthine, which passes into the bloodstream and is not utilized for nucleotide resynthesis by rested muscles [42]. We use a linear approximation to describe both, the degradation of IMP and the efflux of its products from the cell. No measurable loss of purines was reported below the lactate threshold [43], thus the purine nucleotide loss is assumed to be activated only during exercise and set to zero otherwise.

Since the de novo synthesis of IMP is a complex mechanism, it is modeled by an effective equation taking into account the rate-limiting key enzymes. The first regulatory reaction is the ATP dependent transfer of diphosphate to D-ribose 5-phosphate via the enzyme ribose-phosphate diphosphokinase, which is competitively inhibited by ADP [44]. The subsequent committed step of the IMP pathway is the synthesis of 5-Phosphoribosylamin catalyzed by the enzyme amidophosphoribosyltransferase, which is allosterically inhibited by its end products AMP and IMP.

The resynthesis of AMP from IMP catalyzed by the adenylosuccinate synthase is feedback inhibited by its product AMP and consumes one GTP [45,46]. Since Guanosinphosphates are not included in our simulations the GTP concentration is estimated as 14.8% of the ATP concentration [47]. The reported K_m and K_i values differ considerably depending on the organism, tissue type and conditions of assay [45,48,49,46]. There are two types of adenylosuccinate synthase isozymes in mammals of which muscles contain mainly one with a high K_{mIMP} value of 0.2–0.7 mM [45,48–50] compared to its concentration, a K_{mGTP} between

Table 1
Velocities of all model reactions.

Reaction velocity [mM/min]	Parameters
Intramitochondrial reactions [30]	
Substrate dehydrogenase: $v_{DH} = k_{DH} \frac{\text{pyruvate}}{(1 + K_{mN} \frac{NADH}{NAD})^D}$	$k_{DH} = 37.689 \text{ mM min}^{-1}$, $K_{mN} = 100$, $P_D = 0.8$ [30], pyruvate dependence added.
Complex I: $v_{C1} = k_{C1} \cdot \Delta G_{C1}$	$k_{C1} = 0.112 \text{ mM mV}^{-1} \text{ min}^{-1}$.
Complex III: $v_{C3} = k_{C3} \cdot \Delta G_{C3}$	$k_{C3} = 0.521 \text{ mM mV}^{-1} \text{ min}^{-1}$, ΔG_{C3} defined in the Supplementary information.
Complex IV: $v_{C4} = k_{C4} \frac{a^{2+} \cdot c^{2+}}{1 + \frac{K_{mO}}{O_2}}$	$k_{C4} = 1951.98 \text{ mM min}^{-1}$, $K_{mO} = 0.12 \text{ mM}$, $O_2 = 0.24 \text{ mM}$, a^{2+} is the concentration of reduced cytochrome a (Supplementary information).
ATP synthase: $v_{SN} = k_{SN} \frac{\gamma - 1}{\gamma + 1}$	$k_{SN} = 3.034 \text{ mM min}^{-1}$, γ (see Supplementary information).
Mitochondrial exchanges [30]	
Phosphate carrier: $v_{PI} = k_{PI} (R_{H_2PO_4,e} \cdot P_{i,e} \cdot H_e^+ - R_{H_2PO_4,i} \cdot P_{i,i} \cdot H_i^+)$, with $R_{H_2PO_4,e/i} = \frac{1}{1 + 10^{pH_{e/i} - 6.8}}$	$k_{PI} = 9.542 \mu\text{M}^{-1} \text{ min}^{-1}$, $R_{H_2PO_4}$ is the ratio of H_2PO_4 to the total phosphate concentration.
ATP-ADP-translocase: $v_{EX} = \frac{k_{EX}}{1 + \frac{K_{mADP}}{ADP_f}} \cdot \left(\frac{ADP_f}{ADP_f + ATP_f \cdot 10^{0.35\Delta\phi/Z}} - \frac{ADP_{fi}}{ADP_{fi} + ATP_{fi} \cdot 10^{-0.65\Delta\phi/Z}} \right)$	$k_{EX} = 3.508 \text{ mM min}^{-1}$, $K_{mADP} = 0.0035 \text{ mM}$. Definitions of $\Delta\phi$, Z and the calculations of free ATP and ADP can be found in the Supplementary information.
$v_{LK} = k_{LK,1} (e^{k_{LK,2}\Delta p} - 1)$	$k_{LK,1} = 0.072 \mu\text{M min}^{-1}$, $k_{LK,2} = 0.038 \text{ mV}^{-1}$ [30]. $k_{LK,1}$ was set to reproduce the measured proton leak in resting skeletal muscles (50% of the respiration rate [79,30]).
Extramitochondrial reactions of the original model [30,31]	
Proton efflux: $v_{PE} = k_{PE}(7 - pH)$	$k_{PE} = 13.1 \text{ mM min}^{-1}$ [53].
Creatine kinase: $v_{CK} = k_{CK} \cdot ADP \cdot PCr \cdot H^+ - k_{b,CK} \cdot ATP \cdot Cr$	$k_{CK} = 1.9258 \mu\text{M}^{-2} \text{ min}^{-1}$ [30], $k_{b,CK} = 0.00116 \mu\text{M}^{-1} \text{ min}^{-1}$ (calculated from steady state concentration).
Adenylate kinase: $v_{AK} = k_{AK} \cdot ADP_{fe} \cdot ADP_{me} - k_{b,AK} \cdot ATP_{me} \cdot AMP$	$k_{AK} = 862.1 \mu\text{M}^{-1} \text{ min}^{-1}$ [30], $k_{b,AK} = 340.01 \mu\text{M}^{-1} \text{ min}^{-1}$ (calculated from steady state concentration).
ATP consumption: $v_{UT} = k_{UT} \frac{1}{1 + \frac{K_{mATP}}{ATP}}$	$k_{UT} = 0.6865 \text{ M min}^{-1}$, $K_{mATP} = 0.15 \text{ mM}$ [30].
Glycolysis: $v_{glyc} = k_{glyc} \cdot ADP \cdot H_2^+ / H^+$	$k_{glyc} = 2.756 \text{ min}^{-1}$.
Extramitochondrial reactions extending the original model	
AMP deaminase: $v_{AD} = k_{AD} \frac{AMP(7.5 - pH)}{AMP + K_{mAMP} \frac{P_i \cdot ADP_0}{P_{i0} \cdot ADP_{f,myo}}}$	$r_{myo} = 1 + \frac{n}{30}$ (n is the ATP consumption factor). $k_{AD} = 683.0 \text{ mM min}^{-1}$, $K_{mAMP} = 1.0 \text{ mM}$ for the free AMP deaminase enzyme (literature value 0.6–1.0 mM [80,37,40]).
Purine nucleotide loss: $v_{PL} = k_{PL}(IMP - IMP_0)^2$	$k_{PL} = 2.18 \text{ min}^{-1}$.
IMP de novo synthesis: $v_{IS} = k_{IS} \frac{ATP}{1 + \frac{ATP}{K_{mATP}} + \frac{ADP}{K_{iADP}}} \cdot \frac{1}{1 + \frac{AMP}{K_{iAMP}} + \frac{IMP}{K_{iIMP}}}$	$k_{IS} = 0.0485 \text{ min}^{-1}$, $K_{mATP} = 0.014$ [44], $K_{iADP} = 0.01$ [44], $K_{iAMP} = 0.092$ [81], $K_{iIMP} = 0.18$ [81]. If the total adenine nucleotide pool equals the value in rest v_{IS} is set to zero.
AMP synthesis: $v_{AS} = k_{AS} \frac{GTP \cdot IMP}{(1 + \frac{GTP}{K_{mGTP}})(1 + \frac{IMP}{K_{mIMP}} + \frac{AMP}{K_{iAMP}})}$	$k_{AS} = 7.487 \text{ mM min}^{-1}$, $K_{mIMP} = 0.3$, $K_{mGMP} = 0.1$, $K_{iAMP} = 3.0$ (see section Extramitochondrial reactions).
Lactate dehydrogenase: $v_{LA} = k_{LA} \cdot \text{pyruvate} \cdot H^+ - k_{b,LA} \cdot \text{lactate}$	$k_{LA} = 950 \mu\text{M}^{-1} \text{ min}^{-1}$, $k_{b,LA} = 6.34 \text{ min}^{-1}$ (calculated from steady state concentration). NAD/NADH was not included as an extramitochondrial species in our model.
Lactate efflux: $v_{LE} = k_{LE}(\text{lactate} - \text{lactate}_0)$	$k_{LE} = 0.06 \text{ min}^{-1}$ was chosen to reproduce the experimentally observed lactate decline to 70% of the post-exercise concentration after 6 min of recovery [58,82].

0.024–0.38 mM [48–50] and a K_{iAMP} in the range of 0.7–3.0 mM [46,49]. In our simulations we used $K_{mIMP} = 0.3$, $K_{mGMP} = 0.1$ and $K_{iAMP} = 3.0$.

2.3. A detailed simulation of pH kinetics

The dynamic of the H^+ concentration depends on a multiplicity of effects, for most of the simulated enzymatic reactions release or consume protons. In addition to the model of Korzeniewski et al. [30,31], our model takes into account the lactate formation, which consumes one H^+ and thus acts against acidification [51] rather than causing it as it was often misunderstood. As a consequence the proton balance of glycolysis is almost neutral when lactate formation is considered [51]. Thus the cause of acidification during high glycolytic rates is not caused by glycolysis itself but rather by the hydrolysis of ATP, which produces H_2PO_4 . Taking into account the ratio between H_2PO_4 and HPO_4 a fraction of $(1 - R_{H_2PO_4})$ (see Table 1) would release one proton into the cytosol. Similar considerations have to be made for the consumption of three HPO_4 during glycolysis, which causes a release of three $R_{H_2PO_4}$ from the remaining H_2PO_4 in addition to the 1 H^+ already produced in glycolytic reactions when using glycogen [51]. The contributions of glycolysis and ATP hydrolysis are assumed to be compensated during oxidative phosphorylation in the resting state, where the lactate concentration stays constant. The ratio $R_{H_2PO_4}$ also plays a role

for the effect of the mitochondrial phosphate carrier on the H^+ concentration, because it solely transports H_2PO_4 .

Another buffering effect is the deamination of AMP, since one of the products is NH_3 , which most likely binds one proton due to the very small NH_3/NH_4^+ ratio in the physiological pH range. The resynthesis of AMP via the adenylosuccinate synthase, however, produces 2 H^+ and one HPO_4 , which yields a total contribution of $(2 - R_{H_2PO_4})$ protons.

2.4. ATP consumption during exercise and parallel activation

Higher work rates are simulated by increasing the velocity of ATP consumption v_{UT} by a factor n , the magnitude of which can be estimated via experimentally observed ATP synthesis rates from glycolysis, oxidative phosphorylation and creatine kinase. We used an initial ATP consumption value of $n = 300$, corresponding to an ATP turnover rate of 3.35 mM/s, which is similar to experimental values of about 3.5 mM/s [52,53].

Even during a short period of 30 s the maximal power output cannot be maintained, but declines to about 60% of the initial value [52]. Thus in our simulations the ATP consumption starts at a maximal rate of 3.35 mM/s (300 times the value at rest) and decreases linearly to 60% at the end of the exercise (see Fig. 4A). After the 30 s interval we assume

Table 2

Comparison of steady state and post-exercise concentrations between simulation and literature. The post-exercise values are also shown in Fig. 3. To convert dry weight literature data a factor of 4 was used.

Species	Rest concentration [mM]		Post-exercise concentration [mM]	
	Simulation	Literature	Simulation	Literature
ATP	6.0	5.2–6.5 [54,55,61,56,39]	3.96	4.1 [54,55,61,56,39]
ADP	0.0158, calculated from [83]	0.012–0.025 [52,53,39,59,62,84]	0.0778	0.064–0.163 [53,39,62,31]
AMP	$4.64 \cdot 10^{-5}$, calculated from [83]	$1.8 \cdot 10^{-6} - 1.25 \cdot 10^{-4}$ [52,53,39,84]	$1.71 \cdot 10^{-3}$	$6.4 \cdot 10^{-5} - 5.0 \cdot 10^{-3}$ [52,53,39]
IMP	0.027	0.01–0.038 [54–56,39]	1.45	0.88–2.36 [54,55,57,61,56]
Purine nucleotide loss	–	–	0.55	0.35–1.0 [54,57,39,61,56]
Phosphocreatine	20.5	19.3–22.7 [54,55,61,56,39]	3.03	1.9–13.9 [54,55,39,58,57,52,53,61,56]
Creatine	9.0	7.7–11.3 [54,55,58,57,56]	26.47	18.0–29.7 [54,55,58,57,56]
Pyruvate	0.068	0.05–0.24 [84,52,70,58]	0.56	0.45–1.15 [52,63,58]
Pi	4.49	2.9–4.65 [53,58,59,85]	21.3	18.5–32.2 [58,53]
Pi _{in}	16.31	16–16.8 [86,85]	88.6	No ref.
Lactate	1.02	0.95–1.5 [54,39,57,56,70,52]	20.72	17.1–29.8 [54–57,52,58]
ATP _i	7.07	varying [87]	7.84	No ref.
ADP _i	2.83	varying [87]	2.06	No ref.
NADH/NAD ratio	0.188	0.186 [70]	0.69	No ref.
Coenzyme Q10 reduced	59.8%	59.1% [88]	82.2%	No ref.
Cytochrome c reduced	14.9%	15–20% [89]	23.9%	No ref.

the ATP consumption factor to decline exponentially to its resting value with a time constant of $\tau = 5$ s.

Similar to Korzeniewski and Liguzinski [31] we assume a parallel activation of enzymes involved in glycolysis and oxidative phosphorylation, which is modeled by enhancing those reactions by a factor n^p depending on the ATP consumption factor, where p is 0.62 for oxidative phosphorylation and 1.15 for glycolysis. These exponents were changed compared to the original model [31] in order to reproduce the experimentally observed metabolite concentrations after high intensity exercise. The relative magnitude of both exponents was estimated from the observed maximum ratio between glycolytic and oxidative ATP flux of 2.9–4.0 [53,52] and from the amount of lactate accumulation after high intensity exercise (17.1–29.8 mM [54–57,52,58]).

To reproduce a faster, more realistic phosphocreatine recovery, we used a similar approach to that described in [33] with two different factors n for ATP consumption and synthesis during the post-exercise period (Fig. 4A). The decline of the factor for ATP synthesis is slower (time constant $\tau = 25$ s), thus leading to an increased ATP synthesis and a faster phosphocreatine recovery.

Kinetic parameters for the simulation were chosen such that they produce steady state concentrations comparable with values reported in the literature as shown in Table 2.

2.5. Modeling CFS during exercise

Studies concerning the exercise response indicate a lower aerobic ATP synthesis rate in CFS patients. McCully et al. calculated oxidative phosphorylation capacities from phosphocreatine recovery kinetics and obtained values of 73% [2] and 80% [3] as average over the CFS group compared to controls. The individual oxidative phosphorylation capacity also correlated with the severity of symptoms. Another study demonstrated that about half of the CFS group exhibited an abnormal increase in plasma lactate after a sub-anaerobic threshold exercise test [4]. The maximal aerobic ATP synthesis rate of those patients was only 65% compared to controls. A similar value (67%) was reported by Argov et al. [59] in patients with exercise intolerance, although CFS patients were intentionally excluded from the exercise test. But due to the heterogeneity within the CFS patients and a possible overlap with other chronic disorders those groups are hard to distinguish. Additionally, in a stress test for neutrophils of CFS patients, which is not directly comparable with exercise tests, a decreased oxidative phosphorylation capacity (about 66%) compared to controls was reported [5,6]. Interestingly, also the resting ATP levels in neutrophils and the ATP–ADP translocase activity were reduced by a similar amount.

To compare the exercise response in CFS to healthy controls we performed simulations with the parameters listed in Table 2, in which the velocities of all reactions related to oxidative phosphorylation were decreased by multiplying a factor r_{CFS} in the range of 0.6–1.0, where 1.0 corresponds to healthy controls and 0.6 to a very severe deficiency.

3. Results

In the following, we first highlight the main predictions of our model concerning recovery times and proceed to compare the simulation results to experimental data of metabolite concentrations after high intensity exercises. In the last three subsections we discuss the underlying mechanisms of exercise dynamic and the consequences for CFS patients in more detail.

3.1. Recovery times for various exercise scenarios

The main advantage of the presented model is the ability to simulate the recovery period of the total adenine nucleotide pool for various cases of CFS severity, exercise intensity and duration. To predict recovery times for reasonable scenarios in the daily routine of a typical CFS patient, we performed simulations for three exercise cases: a 30 s intensive exercise, a moderate 1 h exercise and two moderate 1 h exercises at an interval of 24 h. Fig. 2A shows the time evolution of the ATP concentration for two days after the exercise started. The species influencing the velocity of IMP de novo synthesis do not change much during recovery, thus the ATP concentration increases almost linearly with a slightly lower slope for CFS simulations. Since the preceding formation of ribose 5-phosphate is thought to set an upper limit on the IMP synthesis rate [60], a linear recovery would also be expected in vivo. The recovery time to 97% of the resting ATP concentration for a CFS case with a mitochondrial capacity of 70% of the healthy group is considerably longer than that of controls (Fig. 2B). Interestingly, our model predicts that a long moderate exercise leads to a recovery period of 49 h, which is prolonged by 17 h compared to a short intensive exercise for CFS patients. For controls the opposite is the case, the recovery times being 10.3 h after a short intensive exercise and 4.5 h after a moderate 1 h exercise. They do not reach such low ATP concentrations, where purine nucleotide loss is inevitable, during moderate exercise. But it should be considered that the very low ATP minimum below 50% of the resting value in CFS simulations would probably lead to cell damage and prevent the CFS patients from maintaining the power output simulated in the 30 s exercise scenario. The simulation of a repeated exercise after 24 h demonstrates that if the long recovery periods are not adhered

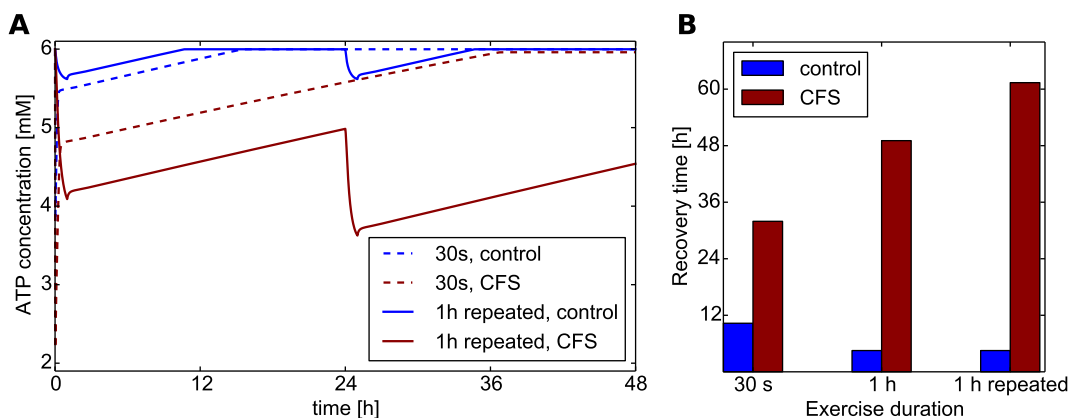


Fig. 2. Recovery from various exercise scenarios. (A) Simulated ATP concentration for CFS patients and controls during exercise and two days of recovery for an intensive 30 s exercise (initial ATP consumption of 300 times the resting value, time dependence shown in Fig. 4A) and a moderate 1 h exercise repeated after 24 h (ATP consumption of 10 times the resting value). (B) Comparison between CFS and control simulations regarding the recovery times after three exercise scenarios: 30 s intensive exercise, 1 h moderate exercise and 1 h repeated exercise after 24 h.

to, it leads to cumulative effects amplifying the symptoms of PEM for recovery times as long as 61 h.

3.2. Comparison of simulations for healthy subjects to experimental data

Here, we compare the results of exercise simulations for healthy subjects with measurements of the metabolite concentrations after 30 s of high intensity exercise. The post-exercise concentrations are listed in Table 2 and shown in Fig. 3 together with experimental data from [54,55,39,58,57,52,53,61,56,62,63]. There is good agreement with experimentally observed metabolite concentrations, which were taken after the same exercise period of 30 s but nevertheless exhibit a wide variation probably due to varying bodily constitution and exercise intensity among individuals. As indicated in the figure, values for measurements after 3 min of exercise are also displayed for comparison.

In Fig. 4C and D time series of important metabolites during and after a 30 s intensive exercise are shown. The concentration ATP decreases and the concentrations ADP, AMP and IMP increase continuously during exercise, because the total ATP synthesis rate is not able to match the

ATP usage completely. The phosphocreatine concentration declines fast to ensure enough power output during the beginning of the exercise and recovers during the first 3 min of rest to about 77% of the resting value similar to reported measurements [58].

The ATP fluxes are depicted in Fig. 4E, where the AMP synthesis and IMP synthesis are excluded because of their negligible contribution. Glycolysis is the major energy source during high intensity training with a maximum ratio between glycolytic and oxidative ATP flux of 2.98, which is in the range of reported values 2.9–4.0 [53,52]. The creatine kinase flux is high during the first seconds but since the phosphocreatine recovery consumes ATP it can only act as a temporary energy storage and thus its contribution declines during exercise. ATP synthesis via adenylate kinase is low compared to the other fluxes, however, its main function is not only to gain additional ATP, but to stabilize the ATP/ADP ratio and thus the Gibbs free energy from ATP hydrolysis.

The high rate of anaerobic glycolysis leads to a decreasing pH value (Fig. 4B) during exercise. The post-exercise acidification of about 0.1 pH unit is due to the fast phosphocreatine recovery, which releases H^+ to the cytosol. Both, the post-exercise acidification as well as the

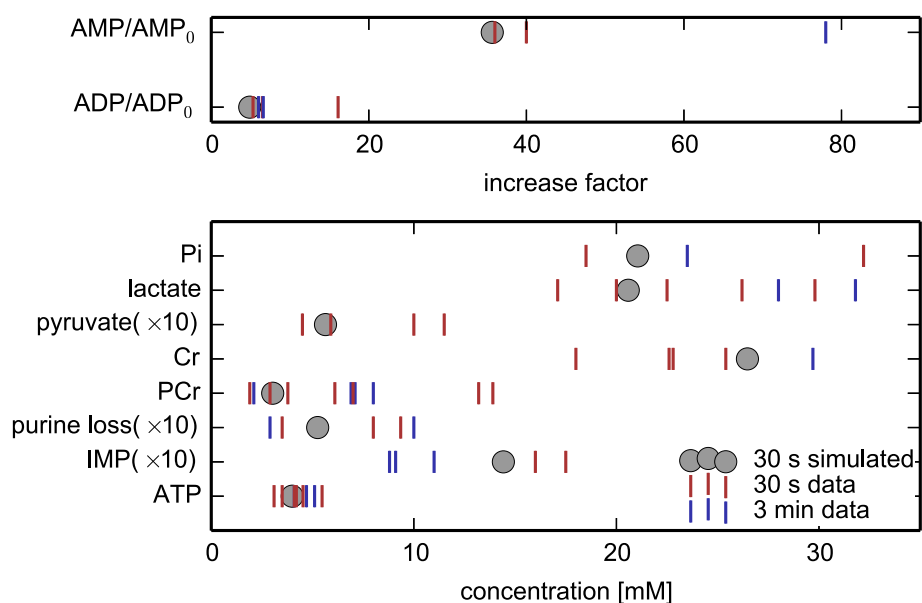


Fig. 3. Species concentrations after 30 s high intensity exercise. Simulated post-exercise concentrations for healthy subjects are compared to measurements from experimental studies, where values after 30 s and 3 min exercises are displayed separately. Literature references are listed in Table 2. To convert dry weight literature data a factor of 4 was used.

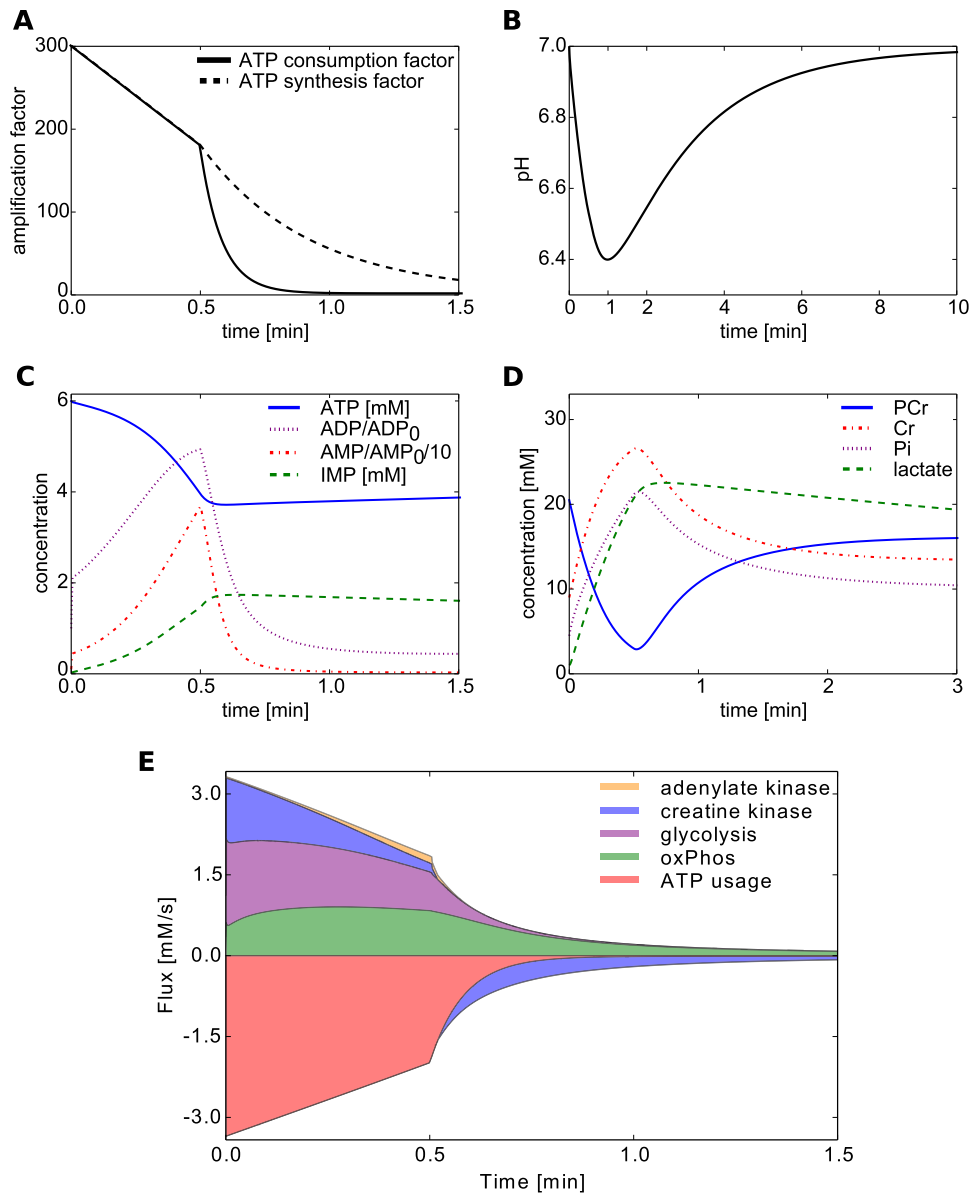


Fig. 4. Simulated exercise kinetics for healthy subjects. (A) ATP consumption factor and ATP synthesis factor for 30 s exercise simulations. (B) pH during exercise. (C) ATP, ADP, AMP and IMP during exercise. For ADP and AMP the increase compared to resting state is plotted, where the factor for AMP is divided by 10. (D) Phosphocreatine, creatine, Pi and lactate. (E) ATP fluxes for the most contributing reactions during exercise and 1 min of recovery. The ATP synthase flux is referred to as "oxPhos".

recovery time (about 6 min to pH 6.9), are in good agreement with measurements of pH kinetics [53].

To identify the most important reactions influencing the dynamic of the system, we performed a global sensitivity analysis regarding the steady state and post-exercise concentrations in dependence of the kinetic parameters. The results of the sensitivity analysis are described in the Supplementary Information section.

3.3. Post-exercise recovery dynamics

In the following, we discuss the mechanisms involved in the exercise induced purine nucleotide degradation and post-exercise recovery of the total adenine pool. The effects of a reduced aerobic ATP synthesis on the recovery dynamics will be considered in the subsequent subsection.

When the ATP demand exceeds the supply during exercise, the adenylate kinase converts two ADP to one ATP and AMP, thereby stabilizing the ATP/ADP ratio and thus the free Gibbs energy gained from ATP

hydrolysis. Due to the high AMP levels and reduced pH the IMP producing activity of the AMP deaminase is upregulated and thereby ensures the stabilizing effect of adenylate kinase to be continued. Furthermore, one H^+ is absorbed during the reaction, which counteracts the advancing acidification, but increases the amount of IMP degraded to inosine and hypoxanthine and finally uric acid. The temporary benefit, which can be essential for survival, comes at a high price the reduction of the total adenine nucleotide pool, the recovery of which can take hours or days of rest. After high energy demand over a long period without sufficient rest even athletic subjects need more than 72 h to replenish their adenine nucleotide pool [64,65].

Using the original model of Korzeniewski et al. [30,31], the recovery is much faster because, without the consideration of purine nucleotide degradation, the total adenine nucleotide pool is a conserved quantity and steady states are reached fast due to the typical time scale of the included reactions. In simulations with the extended model however, the purine nucleotide loss accounts for 9% of the resting ATP concentration for healthy controls, which is consistent with measurements after high

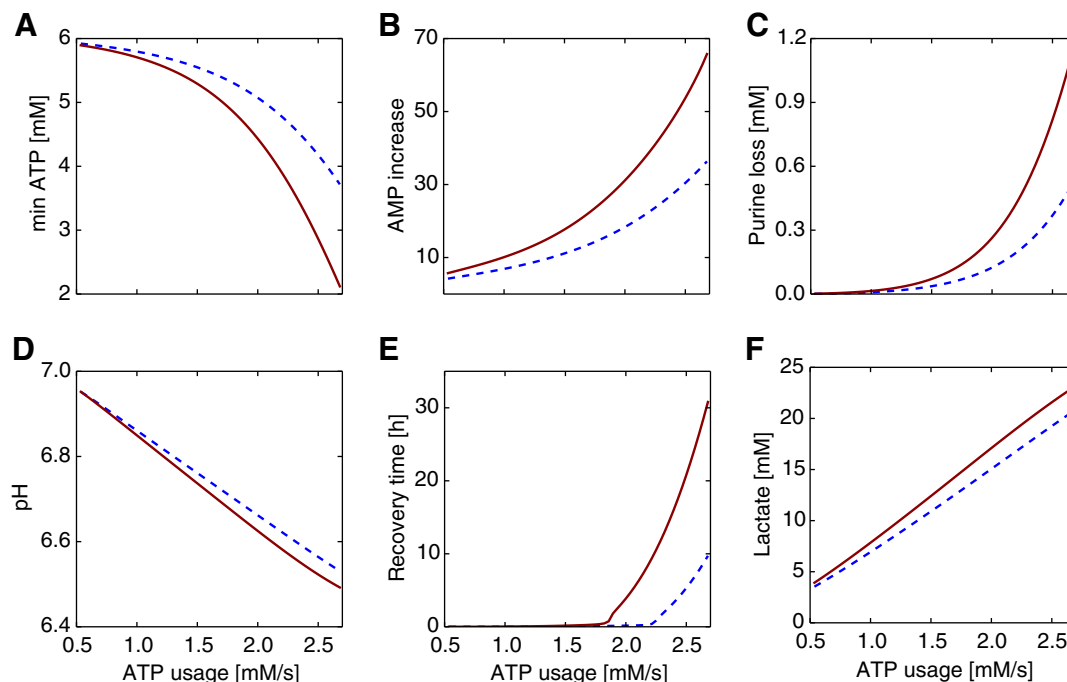


Fig. 5. Post-exercise observables in dependence on the ATP usage. Metabolite concentration after a 30 s exercise of varying intensity (ATP usage) were simulated for controls (blue dashed line) and for CFS patients with $r_{\text{CFS}} = 0.7$ (red solid line). A complete presentation for all CFS factors in the range from 0.6 to 1.0 can be found in Suppl. Fig. 2. (A) ATP minimum during exercise, which should not be confused with the post-exercise value after 30 s, since the ATP level continues to fall during the exponential decay of the ATP consumption factor. (B) Increase of AMP concentration compared to resting value. (C) Purine nucleotide loss due to IMP degradation. (D) Recovery time for the ATP concentration to reach 97% of the resting value. (E) Cytosolic pH minimum during exercise. (F) Lactate accumulation. (For interpretation of the references to color in this figure legend, the reader is referred to the web version of this article.)

intensity exercises [39,54,57]. After 10 h the ATP concentration recovers to 97% of its resting value, which corresponds to a de novo synthesis rate of 0.6% of the total adenine nucleotide pool per hour. The experimentally observed rate of purine de novo synthesis is in the range of 0.3–1.0% per hour [66] containing the simulated value.

3.4. Exercise response and slow recovery in CFS

As described in the last part of the Method section, we performed simulations of various degrees of CFS severity by decreasing the velocity of mitochondrial reactions down to 60% of the control value based on experimental observations [2–4,59,5,6]. Fig. 5 displays various observables for the control case ($r_{\text{CFS}} = 1.0$) and a CFS scenario with mitochondrial capacity of 70% compared to the controls ($r_{\text{CFS}} = 0.7$), whereas the complete results for all CFS factors in the range mentioned are shown in Suppl. Fig. 2. As shown in Fig. 5A and Suppl. Fig. 2A, the reduced capacity

for aerobic ATP synthesis leads to a much lower minimum ATP concentration during exercise. Even during high intensity exercise ATP levels rarely drop below 55% of resting concentrations [54,55,39,58,57,52], therefore CFS patients would probably be prevented from sustaining work rates above 2 mM/s and perform worse compared to controls, as reported in [1–4].

One of the reasons for a reduced power output is the decreasing ATP/ADP ratio, which leads to a thermodynamically less effective conversion of ATP to ADP via hydrolysis. The change in the Gibbs free energy

$$\Delta G = -31.9 \text{ kJ/mol} + RT \ln(\text{ADP} \cdot \text{Pi}/\text{ATP}), \quad (1)$$

can be seen in Fig. 6A which is dependent on the ATP consumption rate and the CFS severity. R refers to the universal gas constant and T to the temperature. Due to the stabilizing effect of the adenylate kinase and AMP deaminase on the ATP/ADP ratio, the difference in the Gibbs free

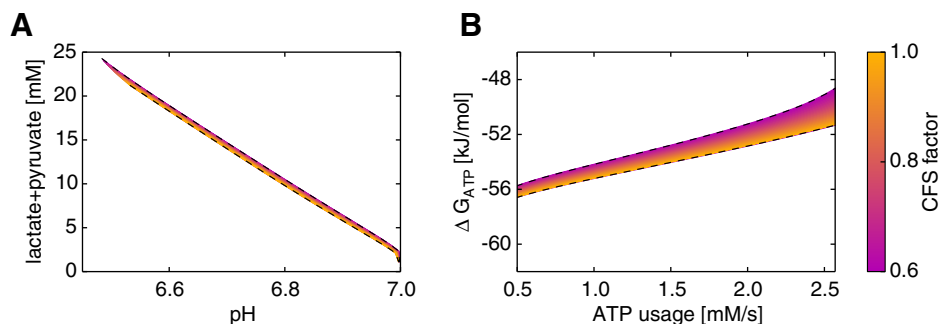


Fig. 6. Lactate accumulation and Gibbs free energy. (A) Linear relationship between lactate concentration and pH. The color gradient displays the effect of different CFS factors. Simulations for CFS patients are shifted up to 0.56 towards lower pH values compared to control simulations with the same ATP consumption, thus causing an apparently thin area in this depiction. (B) Approximately linear relationship between the Gibbs free energy for ATP hydrolysis and the power output. (For interpretation of the references to color in this figure legend, the reader is referred to the web version of this article.)

energy between CFS and controls is less than 3.23 kJ/mol. Jeneson et al. [67] measured a quasi-linear relationship between the Gibbs free energy and the power output, which is compatible with our model, considering the variations of the experimental values.

Stabilizing the ATP/ADP ratio has the adverse effect of producing a considerable higher AMP concentration in CFS simulations compared to simulation for controls (Fig. 5B and Suppl. Fig. 2B). The high AMP concentration then causes an increased purine nucleotide loss (Fig. 5C and Suppl. Fig. 2C), which leads to lower ATP and elevated ADP and AMP post-exercise concentrations. Thus, the *de novo* synthesis of IMP is slowed down by feedback inhibition of key enzymes causing a prolonged recovery time for the total adenine nucleotide pool. 31.9 h of rest is needed to replenish the ATP concentration to 97% of the resting value for a CFS factor of 0.7 (Fig. 5D) and up to 45 h is needed for even lower CFS factors (Suppl. Fig. 2D). Similar to these results, Tullson et al. [66] reported a correlation between the *de novo* synthesis rate and the capacity of oxidative phosphorylation. This mechanism could be one of the reasons for the post-exertional malaise, which typically last for a few days after an exertion beyond the CFS induced energy limits. The delayed recovery has been observed in CFS patients by measuring the force of maximum voluntary contractions, which differed significantly compared to the initial force up to 24 h after exercise [68].

3.5. Acidosis during exercise

As shown in Fig. 5E and Suppl. Fig. 2E, the CFS simulations exhibit an increased acidosis during exercise with a maximal pH difference to the control simulations of 0.056 and a slightly prolonged pH recovery, which concurs with experimental observations [1,25]. As a consequence of the lower pH both, the lactate accumulation (Fig. 5F and Suppl. Fig. 2F) and the lactate efflux from the cell during recovery, were increased up to 15% and 20%, respectively, compared to controls. Both effects were enhanced by reducing the r_{CFS} further. Differences in the lactate accumulation and the anaerobic threshold were also reported in experimental studies [1,4].

The relationship between the accumulated lactate content and the pH was found to be approximately linear in measurements during recovery from exercise [69,51]. Fig. 6 shows that our model also reproduces the reported linearity, fitted by the following function

$$\text{pH} = 0.024(\text{lactate} + \text{pyruvate})/\text{mM} + 7.03, \quad (2)$$

which is similar to the experimental fit of $\text{pH} = 0.0213(\text{lactate} + \text{pyruvate})/\text{nM} + 7.06$ [69,51] when using a dry-to-wet conversion factor of 4.

4. Conclusions

We presented a deterministic model based on rate equations for the relevant reactions and processes to simulate metabolite concentrations during exercise in skeletal muscles and were able to reproduce experimentally observed dynamics during and after a 30 s high intensity exercise [53–55,39,58,57,52,63]. By simulating a reduced mitochondrial ATP synthesis rate for CFS patients the model leads to predictions about the duration of recovery after exertion and demonstrates that long moderate exercises are more exhaustive than short intensive exercises contrary to the results for healthy controls. Furthermore, it was shown that ATP reaches critically low concentrations during high intensity exercise in CFS simulations and the acidification in muscle tissue increases compared to control simulations.

Similar to Korzeniewski and Liguzinski [31] parallel activation of ATP consumption and synthesis was used to model the muscle stimulation. Even though it is a simplistic approach to describe a complex and not yet understood mechanism, there is evidence for a parallel activation *in vivo* [32,70,71].

The reduced mitochondrial capacity in CFS results in an increased acidosis and lactate accumulation, which was not as pronounced as

reported [1,4]. This could be in part explained by the experimental setup of repeated exercise bouts [1] and the heterogeneity of CFS patients, where some possibly exhibit a different parallel activation dynamic with a higher activation of glycolysis.

Investigating the mitochondria in neutrophils of CFS patients, two subgroups have been reported, which have been differentiated by the way the mitochondrial deficiency is compensated [6]. It was proposed that one of the groups compensates the lower aerobic ATP synthesis rate by upregulating glycolysis, the other however, seemed to use an alternative pathway, probably by increasing the purine nucleotide degradation. Our model reproduces the features of both groups and the proportion between both compensatory mechanisms can be changed by modifying the activation dynamic of glycolysis and the kinetics of purine nucleotide degradation. In the simulations presented however, the corresponding parameters were determined by experimental values of healthy subjects.

A major difference between the simulations for healthy controls and CFS patients was the minimum ATP level during exercise, which dropped below 50% of the concentration in rest for workloads higher than 2.45 ATP/s in the CFS simulations. Values below 55% of the resting value have not been measured after high intensity exercise of healthy subjects [54,55,39,58,57,52]. Even if the minimum ATP concentration is still well above the K_m value for most of the ATP-dependent enzymes, a temporary threefold reduction of ATP level has been reported to increase the likelihood for cell death immensely [72]. Thus CFS patients would probably not be able to sustain the power output, and the higher necrosis rates could enhance the symptoms of post-exertional malaise. The level of cell-free DNA in plasma, which is released after necrosis, was increased up to 3.5 times in CFS patients the normal reference value confirming a higher rate of cell death [6]. The amount of cell-free DNA was strongly anti-correlated with the capacity of oxidative phosphorylation indicating that the higher frequency of cell deaths could be the result of ATP concentrations falling below a threshold during exertion. This effect would delay the recovery time, which is already prolonged as our simulations have shown.

Other factors adding to the reduced recovery efficiency are immunological and adrenergic dysregulations [18,19], where the complex interplay with the exercise induced changes in the metabolism are not yet understood. Also oxidative stress was found to be increased after exertion [12] as well as in rest [7–9], which is closely linked to the oxidative phosphorylation capacity since the reduction of major antioxidants such as ubiquinol, coenzyme c and NADH is dependent on mitochondrial respiration.

One effort to shorten the recovery time is to enhance the *de novo* synthesis rate by providing a higher concentration of D-ribose [60], which also proved to be beneficial as supplements to CFS patients [73]. But long-term treatment with D-ribose probably has some drawbacks due to its rapid glycation of proteins, which is involved in physiological neurodegenerative diseases [74]. As long as the pathogenesis of CFS is unclear, a reasonable therapeutic approach is to measure important cofactors for mitochondrial respiration (ubiquinol, NAD, L-carnitine and others) and provide individual supplements [75,76].

To conclude, the presented model is able to reproduce several independent experimental observations and helps to understand the underlying mechanism of exercise intolerance in CFS by taking into account a reduced mitochondrial capacity. The mechanism of post-exercise recovery can be investigated by including the purine nucleotide degradation and loss during exercise into the model. As a consequence of the system dynamics during exercise, the ATP concentration declines to a very low minimum and the purine nucleotide loss increases causing a prolonged recovery time and enhancing the severity of post-exertional malaise.

Supplementary data to this article can be found online at <http://dx.doi.org/10.1016/j.bpc.2015.03.009>.

Authors' contributions

NL: Designed the model, implemented the model, designed the project, and wrote the manuscript.

BD: Designed the project, and wrote the manuscript.

The simulation source code (GPLv3 license) including plot functions is available online at <https://github.com/nleng/ATP-exercise-simulation>.

Acknowledgments

This work was supported by grants from the German Research Council (Graduate college 1657). The funders had no role in the study design, data collection and analysis, decision to publish, or preparation of the manuscript.

References

- [1] D.E. Jones, K.G. Hollingsworth, D.G. Jakovljevic, G. Fattakhova, J. Pairman, A.M. Blamire, M.I. Trenell, J.L. Newton, Loss of capacity to recover from acidosis on repeat exercise in chronic fatigue syndrome: a case–control study, *Eur. J. Clin. Invest.* 42 (2) (2012) 186–194, <http://dx.doi.org/10.1111/j.1365-2362.2011.02567.x>.
- [2] K.K. McCully, B.H. Natelson, S. Iotti, S. Sisto, J.S. Leigh, Reduced oxidative muscle metabolism in chronic fatigue syndrome, *Muscle Nerve* 19 (5) (1996) 621–625, [http://dx.doi.org/10.1002/\(sici\)1097-4598\(199605\)19:5<621::aid-mus10>3.3.co;2-c](http://dx.doi.org/10.1002/(sici)1097-4598(199605)19:5<621::aid-mus10>3.3.co;2-c).
- [3] K.K. McCully, B.H. Natelson, Impaired oxygen delivery to muscle in chronic fatigue syndrome, *Clin. Sci.* 97 (1999) 603–608, <http://dx.doi.org/10.1042/cs19980372>.
- [4] R.J. Lane, M.C. Barrett, D.J. Taylor, G.J. Kemp, R. Lodi, Heterogeneity in chronic fatigue syndrome: evidence from magnetic resonance spectroscopy of muscle, *Neuromuscul. Disord.* 8 (3) (1998) 204–209, [http://dx.doi.org/10.1016/S0960-8966\(98\)00021-2](http://dx.doi.org/10.1016/S0960-8966(98)00021-2).
- [5] S. Myhill, N.E. Booth, J. McLaren-Howard, Chronic fatigue syndrome and mitochondrial dysfunction, *Int. J. Clin. Exp. Med.* 2 (1) (2009) 1.
- [6] N.E. Booth, S. Myhill, J. McLaren-Howard, Mitochondrial dysfunction and the pathophysiology of Myalgic Encephalomyelitis/Chronic Fatigue Syndrome (ME/CFS), *Int. J. Clin. Exp. Med.* 5 (3) (2012) 208.
- [7] S. Fulle, P. Mecocci, G. Fanò, I. Vecchiet, A. Vecchini, D. Racciotti, A. Cherubini, E. Pizzigallo, L. Vecchiet, U. Senin, M.F. Beal, Specific oxidative alterations in vastus lateralis muscle of patients with the diagnosis of chronic fatigue syndrome, *Free Radic. Biol. Med.* 29 (12) (2000) 1252–1259, [http://dx.doi.org/10.1016/S0891-5849\(00\)00419-6](http://dx.doi.org/10.1016/S0891-5849(00)00419-6).
- [8] G. Kennedy, V.A. Spence, M. McLaren, A. Hill, C. Underwood, J.J. Belch, Oxidative stress levels are raised in chronic fatigue syndrome and are associated with clinical symptoms, *Free Radic. Biol. Med.* 39 (5) (2005) 584–589, <http://dx.doi.org/10.1016/j.freeradbiomed.2005.04.020>.
- [9] R. Richards, T. Roberts, N. McGregor, R. Dunstan, H. Butt, Blood parameters indicative of oxidative stress are associated with symptom expression in chronic fatigue syndrome, *Redox Rep.* 5 (1) (2000) 35–41, <http://dx.doi.org/10.1179/rer.2000.5.1.35>.
- [10] J. Van Oosterwijck, J. Nijs, M. Meeus, I. Lefever, L. Huybrechts, L. Lambrecht, L. Paul, Pain inhibition and postexertional malaise in myalgic encephalomyelitis/chronic fatigue syndrome: an experimental study, *J. Intern. Med.* 268 (3) (2010) 265–278, <http://dx.doi.org/10.1111/j.1365-2796.2010.02228.x>.
- [11] J.M. VanNess, S.R. Stevens, L. Bateman, T.L. Stiles, C.R. Snell, Postexertional malaise in women with chronic fatigue syndrome, *J. Women's Health* 19 (2) (2010) 239–244, <http://dx.doi.org/10.1089/jwh.2009.1507>.
- [12] Y. Jammes, J. Steinberg, O. Mambri, F. Bregeon, S. Delliaux, Chronic fatigue syndrome: assessment of increased oxidative stress and altered muscle excitability in response to incremental exercise, *J. Intern. Med.* 257 (3) (2005) 299–310, <http://dx.doi.org/10.1111/j.1365-2796.2005.01452.x>.
- [13] C. Zhang, A. Baumer, I.R. Mackay, A.W. Linnane, P. Nagley, Unusual pattern of mitochondrial dna deletions in skeletal muscle of an adult human with chronic fatigue syndrome, *Hum. Mol. Genet.* 4 (4) (1995) 751–754, <http://dx.doi.org/10.1093/hmg/4.4.751>.
- [14] J.M. VanNess, C.R. Snell, D.R. Strayer, L. Dempsey, S.R. Stevens, Subclassifying chronic fatigue syndrome through exercise testing, *Med. Sci. Sports Exerc.* 35 (6) (2003) 908–913, <http://dx.doi.org/10.1249/01.mss.0000069510.58763.e8>.
- [15] F. Twisk, M. Maes, A review on cognitive behavioral therapy (CBT) and graded exercise therapy (get) in myalgic encephalomyelitis (ME)/chronic fatigue syndrome (CFS): CBT/GET is not only ineffective and not evidence-based, but also potentially harmful for many patients with ME/CFS, *Neuroendocrinol. Lett.* 30 (3) (2008) 284–299.
- [16] T. Kindlon, Reporting of harms associated with graded exercise therapy and cognitive behavioural therapy in myalgic encephalomyelitis/chronic fatigue syndrome, *Bull. IACFS/ME* 19 (2) (2011) 59–111.
- [17] M. Núñez, J. Fernández-Solà, E. Núñez, J.-M. Fernández-Huerta, T. Godás-Sieso, E. Gomez-Gil, Health-related quality of life in patients with chronic fatigue syndrome: group cognitive behavioural therapy and graded exercise versus usual treatment. A randomised controlled trial with 1 year of follow-up, *Clin. Rheumatol.* 30 (3) (2011) 381–389, <http://dx.doi.org/10.1007/s10067-010-1677-y>.
- [18] A.R. Light, A.T. White, R.W. Hughen, K.C. Light, Moderate exercise increases expression for sensory, adrenergic, and immune genes in chronic fatigue syndrome patients but not in normal subjects, *J. Pain* 10 (10) (2009) 1099–1112, <http://dx.doi.org/10.1016/j.jpain.2009.06.003>.
- [19] A.T. White, A.R. Light, R.W. Hughen, T.A. VanHaitsma, K.C. Light, Differences in metabolite-detecting, adrenergic, and immune gene expression after moderate exercise in patients with chronic fatigue syndrome, patients with multiple sclerosis, and healthy controls, *Psychosom. Med.* 74 (1) (2012) 46–54, <http://dx.doi.org/10.1097/PSY.0b013e31824152ed>.
- [20] K. Fukuda, S.E. Straus, I. Hickie, M.C. Sharpe, J.G. Dobbins, A. Komaroff, The chronic fatigue syndrome: a comprehensive approach to its definition and study, *Ann. Intern. Med.* 121 (12) (1994) 953–959, <http://dx.doi.org/10.7326/0003-4819-121-12-199412150-00009>.
- [21] B.M. Carruthers, A.K. Jain, K.L. De Meirleir, D.L. Peterson, N.G. Klimas, A.M. Lerner, A.C. Bested, P. Flor-Henry, P. Joshi, A.P. Powles, Myalgic encephalomyelitis/chronic fatigue syndrome: clinical working case definition, diagnostic and treatment protocols, *J. Chronic Fatigue Syndr.* 11 (1) (2003) 7–115.
- [22] E.W. Clayton, Beyond Myalgic Encephalomyelitis/Chronic Fatigue Syndrome: An IOM Report on Redefining an Illness, Institute of Medicine of the National Academies, 2015.
- [23] C.R. Snell, S.R. Stevens, T.E. Davenport, J.M. Van Ness, Discriminative validity of metabolic and workload measurements for identifying people with chronic fatigue syndrome, *Theor. Biol. Med. Model.* 93 (11) (2013) 1484–1492, <http://dx.doi.org/10.2522/ptj.20110368>.
- [24] J.M. VanNess, C.R. Snell, S.R. Stevens, L. Bateman, B.A. Keller, Using serial cardiopulmonary exercise tests to support a diagnosis of chronic fatigue syndrome, *Med. Sci. Sports Exerc.* 38 (5) (2006) S85, <http://dx.doi.org/10.1249/00005768-200605001-00386>.
- [25] D. Arnold, G. Radda, P. Bore, P. Styles, D. Taylor, Excessive intracellular acidosis of skeletal muscle on exercise in a patient with a post-viral exhaustion/fatigue syndrome: a 31p nuclear magnetic resonance study, *Lancet* 323 (8391) (1984) 1367–1369, [http://dx.doi.org/10.1016/S0140-6736\(84\)91871-3](http://dx.doi.org/10.1016/S0140-6736(84)91871-3).
- [26] S.D. Vernon, T. Whistler, B. Cameron, I.B. Hickie, W.C. Reeves, A. Lloyd, Preliminary evidence of mitochondrial dysfunction associated with post-infective fatigue after acute infection with epstein barr virus, *BMC Infect. Dis.* 6 (1) (2006) 15.
- [27] P. Englebienne, K. De Meirleir, Chronic Fatigue Syndrome: A Biological Approach, CRC Press, 2002, <http://dx.doi.org/10.1201/9781420041002>.
- [28] Y.-j. Geng, G.K. Hansson, E. Holme, Interferon-gamma and tumor necrosis factor synergize to induce nitric oxide production and inhibit mitochondrial respiration in vascular smooth muscle cells, *Circ. Res.* 71 (5) (1992) 1268–1276, <http://dx.doi.org/10.1161/01.res.71.5.1268>.
- [29] J. Nijs, M. Meeus, N.R. McGregor, R. Meeusen, G. de Schutter, E. van Hoof, K. De Meirleir, Chronic fatigue syndrome: exercise performance related to immune dysfunction, *Med. Sci. Sports Exerc.* 37 (10) (2005) 1647, <http://dx.doi.org/10.1249/01.mss.0000181680.35503.ce>.
- [30] B. Korzeniewski, J.A. Zoladz, A model of oxidative phosphorylation in mammalian skeletal muscle, *Biophys. Chem.* 92 (1) (2001) 17–34, [http://dx.doi.org/10.1016/S0301-4622\(01\)00184-3](http://dx.doi.org/10.1016/S0301-4622(01)00184-3).
- [31] B. Korzeniewski, P. Liguzinski, Theoretical studies on the regulation of anaerobic glycolysis and its influence on oxidative phosphorylation in skeletal muscle, *Biophys. Chem.* 110 (1) (2004) 147–169, <http://dx.doi.org/10.1016/j.bpc.2004.01.011>.
- [32] B. Korzeniewski, V. Deschodt-Arsac, G. Calmettes, J. Franconi, P. Diolet, Physiological heart activation by adrenaline involves parallel activation of ATP usage and supply, *Biochem. J.* 413 (2008) 343–347, <http://dx.doi.org/10.1042/bj20080162>.
- [33] B. Korzeniewski, Regulation of oxidative phosphorylation in different muscles and various experimental conditions, *Biochem. J.* 375 (2003) 799–804, <http://dx.doi.org/10.1042/bj20030882>.
- [34] M. Vendelin, O. Kongas, V. Saks, Regulation of mitochondrial respiration in heart cells analyzed by reaction–diffusion model of energy transfer, *Am. J. Physiol. Cell Physiol.* 278 (4) (2000) C747–C764.
- [35] S. Matsuoaka, N. Sarai, H. Jo, A. Noma, Simulation of ATP metabolism in cardiac excitation–contraction coupling, *Prog. Biophys. Mol. Biol.* 85 (2) (2004) 279–299, <http://dx.doi.org/10.1016/j.pbiomolbio.2004.01.006>.
- [36] J.M. Berg, J.L. Tymoczko, L. Stryer, Biochemistry, 5th edition, 2002.
- [37] A. Raggi, M. Ranieri-Raggi, Regulatory properties of AMP deaminase isoenzymes from rabbit red muscle, *Biochem. J.* 242 (1987) 875–879.
- [38] T.J. Wheeler, J.M. Lowenstein, Adenylate deaminase from rat muscle. Regulation by purine nucleotides and orthophosphate in the presence of 150 mM KCl, *J. Biol. Chem.* 254 (18) (1979) 8994–8999.
- [39] Y. Hellsten, E.A. Richter, B. Kiens, J. Bangsbo, AMP deamination and purine exchange in human skeletal muscle during and after intense exercise, *J. Physiol.* 520 (3) (1999) 909–920, <http://dx.doi.org/10.1111/j.1469-7793.1999.00909.x>.
- [40] K.W. Rundell, P.C. Tullson, R.L. Terjung, Altered kinetics of AMP deaminase by myosin binding, *Am. J. Physiol.* 263 (1992) C294–C299.
- [41] K.W. Rundell, P.C. Tullson, R.L. Terjung, AMP deaminase binding in contracting rat skeletal muscle, *Am. J. Physiol.* 263 (1992) C287–C293, <http://dx.doi.org/10.1249/00005768-199004000-00038>.
- [42] Y. Hellsten, B. Sjödin, E.A. Richter, J. Bangsbo, Urate uptake and lowered ATP levels in human muscle after high-intensity intermittent exercise, *Am. J. Physiol. Endocrinol. Metab.* 274 (4) (1998) E600–E606.
- [43] M.A. Febbraio, J. Dancy, Skeletal muscle energy metabolism during prolonged, fatiguing exercise, *J. Appl. Physiol.* 87 (6) (1999) 2341–2347.
- [44] I.H. Fox, W.N. Kelley, Human phosphoribosylpyrophosphate synthetase distribution, purification, and properties, *J. Biol. Chem.* 246 (18) (1971) 5739–5748.
- [45] G. Van den Bergh, F. Bontemps, M. Vincent, F. Van den Bergh, The purine nucleotide cycle and its molecular defects, *Prog. Neurobiol.* 39 (5) (1992) 547–561, [http://dx.doi.org/10.1016/0301-0082\(92\)90006-z](http://dx.doi.org/10.1016/0301-0082(92)90006-z).
- [46] T. Borza, C.V. Iancu, E. Pike, R.B. Honzatko, H.J. Fromm, Variations in the response of mouse isozymes of adenylosuccinate synthetase to inhibitors of physiological

- relevance, *J. Biol. Chem.* 278 (9) (2003) 6673–6679, <http://dx.doi.org/10.1074/jbc.M210838200>.
- [47] T.W. Traut, Physiological concentrations of purines and pyrimidines, *Mol. Cell. Biochem.* 140 (1) (1994) 1–22, <http://dx.doi.org/10.1007/bf00928361>.
- [48] T. Spector, R.L. Miller, Mammalian adenylsuccinate synthetase: nucleotide monophosphate substrates and inhibitors, *Biochim. Biophys. Acta (BBA) Enzymol.* 445 (2) (1976) 509–517.
- [49] Y. Matsuda, H. Ogawa, S. Fukutome, H. Shiraki, H. Nakagawa, Adenylsuccinate synthetase in rat liver: the existence of two types and their regulatory roles, *Biochem. Biophys. Res. Commun.* 78 (2) (1977) 766–771, [http://dx.doi.org/10.1016/0006-291x\(77\)90245-5](http://dx.doi.org/10.1016/0006-291x(77)90245-5).
- [50] H. Ogawa, H. Shiraki, Y. Matsuda, K. Kakiuchi, H. Nakagawa, Purification, crystallization, and properties of adenylsuccinate synthetase from rat skeletal muscle, *J. Biochem.* 81 (4) (1977) 859–869.
- [51] R.A. Robergs, F. Ghiasvand, D. Parker, Biochemistry of exercise-induced metabolic acidosis, *Am. J. Physiol. Regul. Integr. Comp. Physiol.* 287 (3) (2004) R502–R516, <http://dx.doi.org/10.1152/ajpregu.00114.2004>.
- [52] M.L. Parolin, A. Chesley, M.P. Matsos, L.L. Spriet, N.L. Jones, G.J. Heigenhauser, Regulation of skeletal muscle glycogen phosphorylase and PDH during maximal intermittent exercise, *Am. J. Physiol.* 277 (5 Pt 1) (1999) E890–E900.
- [53] G. Walter, K. Vandeborne, M. Elliott, J.S. Leigh, In vivo ATP synthesis rates in single human muscles during high intensity exercise, *J. Physiol.* 519 (Pt 3) (1999) 901–910, <http://dx.doi.org/10.1111/j.1469-7793.1999.0901n.x>.
- [54] M. Hargreaves, M.J. McKenna, D.G. Jenkins, S.A. Warmington, J.L. Li, R.J. Snow, M.A. Febbraio, Muscle metabolites and performance during high-intensity, intermittent exercise, *J. Appl. Physiol.* 84 (5) (1998) 1687–1691.
- [55] B. Norman, R.L. Sabina, E. Jansson, Regulation of skeletal muscle ATP catabolism by AMPD1 genotype during sprint exercise in asymptomatic subjects, *J. Appl. Physiol.* 91 (1) (2001) 258–264.
- [56] P.C. Tullson, J. Bangsbo, Y. Hellsten, E.A. Richter, Metabolism in human skeletal muscle after exhaustive exercise, *J. Appl. Physiol.* 78 (1) (1995) 146–152.
- [57] S. Zhao, R. Snow, C. Stathis, M. Febbraio, M. Carey, Muscle adenine nucleotide metabolism during and in recovery from maximal exercise in humans, *J. Appl. Physiol.* 88 (5) (2000) 1513–1519.
- [58] G.C. Bogdanis, M.E. Nevill, L.H. Boobis, H. Lakomy, A.M. Nevill, Recovery of power output and muscle metabolites following 30 s of maximal sprint cycling in man, *J. Physiol.* 482 (Pt 2) (1995) 467–480, <http://dx.doi.org/10.1111/jphysiol.1995.sp020533>.
- [59] Z. Argov, N. De Stefano, T. Taivassalo, J. Chen, G. Karpati, D. Arnold, Abnormal oxidative metabolism in exercise intolerance of undetermined origin, *Neuromuscul. Disord.* 7 (2) (1997) 99–104, [http://dx.doi.org/10.1016/S0960-8966\(97\)00426-4](http://dx.doi.org/10.1016/S0960-8966(97)00426-4).
- [60] P.C. Tullson, R.L. Terjung, Adenine nucleotide synthesis in exercising and endurance-trained skeletal muscle, *Am. J. Physiol.* 261 (2 Pt 1) (1991) C342–C347.
- [61] T.E. Graham, J. Bangsbo, P.D. Gollnick, C. Juel, B. Saltin, Ammonia metabolism during intense dynamic exercise and recovery in humans, *Am. J. Physiol.* 259 (2 Pt 1) (1990) E170–E176.
- [62] J. Zoladz, B. Korzeniewski, P. Kulinowski, J. Zapart-Bukowska, J. Majerczak, A. Jasinski, Phosphocreatine recovery overshoot after high intensity exercise in human skeletal muscle is associated with extensive muscle acidification and a significant decrease in phosphorylation potential, *J. Physiol. Sci.* 60 (5) (2010) 331–341, <http://dx.doi.org/10.1007/s12576-010-0101-3>.
- [63] L.L. Spriet, M.I. Lindinger, R.S. McKelvie, G.J. Heigenhauser, N.L. Jones, Muscle glycogenolysis and H⁺ concentration during maximal intermittent cycling, *J. Appl. Physiol.* 66 (1) (1989) 8–13.
- [64] Y. Hellsten, L. Skadhauge, J. Bangsbo, Effect of ribose supplementation on resynthesis of adenine nucleotides after intense intermittent training in humans, *Am. J. Physiol. Regul. Integr. Comp. Physiol.* 286 (1) (2004) R182–R188, <http://dx.doi.org/10.1152/ajpregu.00286.2003>.
- [65] Y. Hellsten-Westling, B. Norman, P.D. Balsom, B. Sjödén, Decreased resting levels of adenine nucleotides in human skeletal muscle after high-intensity training, *J. Appl. Physiol.* 74 (1993) 2523–2528.
- [66] P.C. Tullson, H.B. John-Alder, D.A. Hood, R.L. Terjung, De novo synthesis of adenine nucleotides in different skeletal muscle fiber types, *Am. J. Physiol.* 255 (3 Pt 1) (1988) C271–C277.
- [67] J. Jeneson, H. Westerhoff, T. Brown, C. Van Echteld, R. Berger, Quasi-linear relationship between Gibbs free energy of ATP hydrolysis and power output in human forearm muscle, *Am. J. Physiol. Cell Physiol.* 37 (6) (1995) C1474.
- [68] L. Paul, L. Wood, W.M. Behan, W.M. Maclaren, Demonstration of delayed recovery from fatiguing exercise in chronic fatigue syndrome, *Eur. J. Neurol.* 6 (1) (1999) 63–69, <http://dx.doi.org/10.1046/j.1468-1331.1999.610063.x>.
- [69] K. Sahlin, R.C. Harris, E. Hultman, Creatine kinase equilibrium and lactate content compared with muscle pH in tissue samples obtained after isometric exercise, *Biochem. J.* 152 (1975) 173–180.
- [70] L. Zhou, M.E. Cabrera, H. Huang, C.L. Yuan, D.K. Monika, N. Sharma, F. Bian, W.C. Stanley, Parallel activation of mitochondrial oxidative metabolism with increased cardiac energy expenditure is not dependent on fatty acid oxidation in pigs, *J. Physiol.* 579 (Pt 3) (2007) 811–821, <http://dx.doi.org/10.1113/jphysiol.2006.123828>.
- [71] P.R. Territo, S.A. French, M.C. Dunleavy, F.J. Evans, R.S. Balaban, Calcium activation of heart mitochondrial oxidative phosphorylation rapid kinetics of mVO₂, NADH, and light scattering, *J. Biol. Chem.* 276 (4) (2001) 2586–2599, <http://dx.doi.org/10.1074/jbc.M002923200>.
- [72] D.S. Izumov, A.V. Avetisyan, O.Y. Pletjushkina, D.V. Sakharov, K.W. Wirtz, B.V. Chernyak, V.P. Skulachev, “Wages of fear”: transient threefold decrease in intracellular ATP level imposes apoptosis, *Biochim. Biophys. Acta (BBA) Bioenerg.* 1658 (1) (2004) 141–147, <http://dx.doi.org/10.1016/j.bbabi.2004.05.007>.
- [73] J.E. Teitelbaum, C. Johnson, J.S. Cyr, The use of D-ribose in chronic fatigue syndrome and fibromyalgia: a pilot study, *J. Altern. Complement. Med.* 12 (9) (2006) 857–862, <http://dx.doi.org/10.1089/acm.2006.12.857>.
- [74] Y. Wei, L. Chen, J. Chen, L. Ge, R.Q. He, Rapid glycation with D-ribose induces globular amyloid-like aggregations of BSA with high cytotoxicity to SH-SY5Y cells, *BMC Cell Biol.* 10 (1) (2009) 10, <http://dx.doi.org/10.1186/1471-2121-10-10>.
- [75] S. Myhill, N.E. Booth, J. McLaren-Howard, Targeting mitochondrial dysfunction in the treatment of myalgic encephalomyelitis/chronic fatigue syndrome (ME/CFS)—a clinical audit, *Int. J. Clin. Exp. Med.* 6 (1) (2013) 1.
- [76] L.M. Forsyth, H.G. Preuss, A.L. MacDowell, L. Chiazze Jr., G.D. Birkmayer, J.A. Bellanti, Therapeutic effects of oral NADH on the symptoms of patients with chronic fatigue syndrome, *Ann. Allergy Asthma Immunol.* 82 (2) (1999) 185–191, [http://dx.doi.org/10.1016/s1081-1206\(10\)62595-1](http://dx.doi.org/10.1016/s1081-1206(10)62595-1).
- [77] E. Borgonovo, A new uncertainty importance measure, *Reliab. Eng. Syst. Saf.* 92 (6) (2007) 771–784, <http://dx.doi.org/10.1016/j.res.2006.04.015>.
- [78] E. Plischke, E. Borgonovo, C.L. Smith, Global sensitivity measures from given data, *Eur. J. Oper. Res.* 226 (3) (2013) 536–550, <http://dx.doi.org/10.1016/j.ejor.2012.11.047>.
- [79] D.F. Rolfe, M.D. Brand, Contribution of mitochondrial proton leak to skeletal muscle respiration and to standard metabolic rate, *Am. J. Physiol. Cell Physiol.* 40 (4) (1996) C1380.
- [80] M.T. Bauschjirken, R.L. Sabina, Divergent n-terminal regions in AMP deaminase and isoform-specific catalytic properties of the enzyme, *Arch. Biochem. Biophys.* 321 (2) (1995) 372–380.
- [81] C.T. Caskey, D.M. Ashton, J.B. Wyngaarden, The enzymology of feedback inhibition of glutamine phosphoribosylpyrophosphate amidotransferase by purine ribonucleotides, *J. Biol. Chem.* 239 (8) (1964) 2570–2579.
- [82] K. Sahlin, R. Harris, B. Nylinde, E. Hultman, Lactate content and pH in muscle samples obtained after dynamic exercise, *Pflügers Arch.* 367 (2) (1976) 143–149, <http://dx.doi.org/10.1007/bf00585150>.
- [83] G.J. Kemp, M. Rousell, D. Bendahan, Y.L. Fur, P.J. Cozzzone, Interrelations of ATP synthesis and proton handling in ischaemically exercising human forearm muscle studied by ³¹P magnetic resonance spectroscopy, *J. Physiol.* 535.3 (2001) 901–928, <http://dx.doi.org/10.1111/j.1469-7793.2001.00901.x>.
- [84] T. Stellingwerff, P.J. Leblanc, M.G. Hollidge, G.J.F. Heigenhauser, L.L. Spriet, Hyperoxia decreases muscle glycogenolysis, lactate production, and lactate efflux during steady-state exercise, *Am. J. Physiol. Endocrinol. Metab.* 290 (6) (2006) E1180–E1190, <http://dx.doi.org/10.1152/ajpendo.00499.2005>.
- [85] T.P.M. Akerboom, H. Bookelman, P.F. Zuurendonk, Intramitochondrial and extramitochondrial concentrations of adenine nucleotides and inorganic phosphate in isolated hepatocytes from fasted rats, *J. Biochem.* 84 (1978) 413–420, <http://dx.doi.org/10.1111/j.1432-1033.1978.tb12182.x>.
- [86] F. Brawand, G. Folly, P. Walter, Relation between extra- and intramitochondrial ATP/ADP ratios in rat liver mitochondria, *Biochim. Biophys. Acta* 590 (1979) 285–289, [http://dx.doi.org/10.1016/0005-2728\(80\)90199-1](http://dx.doi.org/10.1016/0005-2728(80)90199-1).
- [87] E. Metelkin, O. Demin, Z. Kovács, C. Chinopoulos, Modeling of ATP–ADP steady-state exchange rate mediated by the adenine nucleotide translocase in isolated mitochondria, *FEBS J.* 276 (23) (2009) 6942–6955, <http://dx.doi.org/10.1111/j.1742-4658.2009.07394.x>.
- [88] L. Miles, M.V. Miles, P.H. Tang, P.S. Horn, J.G. Quinlan, B. Wong, A. Wenisch, K.E. Bove, Ubiquinol: a potential biomarker for tissue energy requirements and oxidative stress, *Clin. Chim. Acta* 360 (1) (2005) 87–96, <http://dx.doi.org/10.1016/j.cccn.2005.04.009>.
- [89] T. Kashiwagura, D.F. Wilson, M. Erecińska, Oxygen dependence of cellular metabolism: the effect of O₂ tension on gluconeogenesis and urea synthesis in isolated rat hepatocytes, *J. Cell. Physiol.* 120 (1) (1984) 13–18, <http://dx.doi.org/10.1002/jcp.1041200103>.